Metal film on a substrate: Dynamics under the action of ultrashort laser pulse

You may also be interested in:

Blistering of film from substrate after action of ultrashort laser pulse
N A Inogamov, V V Zhakhovsky, V A Khokhlov et al.

Adiabatic approximations for electrons interacting with ultrashort high-frequency laser pulses
Koudai Toyota, Ulf Saalmann and Jan M Rost

Photoionization of Rydberg States by Ultrashort Wavelet Pulses
S Yu Svita and V A Astapenko

Double ionization of molecule H2 in intense ultrashort laser fields
Thu-Thuy Le and Ngoc-Ty Nguyen

Characteristics of the damage of transparent solids byultrashort laser pulses
V A Gridin, A N Petrovskii and S L Pestmal

Dynamics of laser ablation at the early stage during and after ultrashort pulse
D K Ilnitsky, V A Khokhlov, V V Zhakhovsky et al.

Writing of 3D optical integrated circuits with ultrashort laser pulses in the presence of strong spherical aberration
M A Bukharin, N N Skryabin, D V Khudyakov et al.

Metal film on a substrate: Dynamics under the action of ultrashort laser pulse

V A Khokhlov[1]**, V V Zhakhovsky**[2,3,1]**, K V Khishchenko**[3]**,
N A Inogamov**[1] **and S I Anisimov**[1]

[1] Landau Institute for Theoretical Physics of the Russian Academy of Scienses, Akademika Semenova 1a, Chernogolovka, Moscow Region 142432, Russia
[2] Dukhov Research Institute of Automatics (VNIIA), Luganskaya 9, Moscow 115304, Russia
[3] Joint Institute for High Temperatures of the Russian Academy of Sciences, Izhorskaya 13 Bldg 2, Moscow 125412, Russia

E-mail: v_a_kh@mail.ru

Abstract. The movement of metal film placed on a glass substrate under action of ultra-short laser pulse is studied with using of two-temperature hydrodynamic calculations. The features of the oscillatory modes of movement of the film on the substrate under the influence of low-energy laser pulses are investigated. Transition from film delamination from the substrate as a whole to break of a film and flying away only a forward layer of a film is tracked at growth of the enclosed energy.

1. Introduction

Many laser experiments have been performed using the targets made up of metallic film mounted on a dielectric or semiconductor substrate. Therefore, the problem of such targets dynamics under the pulsed laser action is significant. In the literature, the bulk targets [1–5] or freestanding films [6–11] are considered mainly. These two cases differ qualitatively from the film–substrate case considered here. In the bulk targets, the phenomenon of the rear-side spallation is absent. In the freestanding films (vacuum from both sides), there is no dynamic influence from the substrate. The parameter d_f/d_t and absorbed fluence F_{abs} parameterize dynamics of ablation (irradiated side) and spallation (rear-side) of the freestanding film [11], here d_f and d_t are thicknesses of a film and a heat affected layer.

Previously [12], the oscillations and the separation of a thin ($d_f < d_t$) film *as a whole* from the substrate have been studied. In the present paper, we consider, firstly, the features of the oscillatory modes of movement of the film on the substrate under the influence of low-energy laser pulses and, secondly, transition from the regime of separation a film as whole to the regime of the internal breaking of a film. If a film is thick ($d_f > d_t$), two breakings appear (if $F > F_{spall} > F_{abl}$), here F_{spall} and F_{abl} are the spallation and ablation thresholds, respectively. The first breaking is ablation near the film–substrate contact, while the second breaking is a spallation in the rarefaction wave at rear side. In the thin films these two breakings merge together [11].

2. 2T hydrodynamics

The following results were obtained using two-temperature hydrodynamic simulation model. In this model, the hydrodynamics is considered uniform under the influence of the total pressure $P = P_{\mathrm{e}} + P_{\mathrm{i}}$, and the thermodynamics is considered separately for the ionic and electronic subsystems.

In metals, the electron–electron thermal relaxation time, as well as the ion–ion (in solid there is phonon–phonon) relaxation time is much shorter than the time of electron–phonon temperature equilibration. Because of this a metal can be considered as a quasi-equilibrium system during the time smaller than the electron–ion (electron–phonon) relaxation time. Such is the case when electrons are heated by an ultra short laser pulse [13]. A metal is considered as a quasi-equilibrium system characterized by two temperatures, ion (lattice) temperature T_{i} and electron temperature T_{e}.

Let us consider that, in the space of two temperatures, it is possible to enter coordinates, with sufficient accuracy globally orthogonal in all interesting area of parameters: $F(T_1, T_2) = F_1(T_1) + F_2(T_2)$, and cross members are negligible small. Then in the thermal balance equation, for simplicity in a one-dimensional case and without a thermal source it is possible to collect separately the terms relating to each of the subsystems 1 and 2:

$$\left\{ \rho \dot{E}_1(x_0, t) - \frac{\partial}{\partial x}\left(\kappa_1 \frac{\partial T_1}{\partial x} \right) + P_1 \frac{\partial v}{\partial x} \right\} + \left\{ \rho \dot{E}_2(x_0, t) - \frac{\partial}{\partial x}\left(\kappa_2 \frac{\partial T_2}{\partial x} \right) + P_2 \frac{\partial v}{\partial x} \right\} = 0. \quad (1)$$

Here x and x_0 are current coordinate and coordinate in connected with substance (Lagrangian) frame.

Usually, the phonon energy flux does not depend on T_{e} and is much smaller than the energy flux connected with electrons. Assuming that κ_1 is independent of the T_2, we obtain that the terms in the first brace do not depend on the T_2, and in the first theirs can only be a parametric dependence κ_2 of the T_1. This permits to split general equation of energy balance into two equations for two subsystems (including the energy exchange between the subsystems):

$$\rho \dot{E}_1(x_0, t) - \frac{\partial}{\partial x}\left(\kappa_1 \frac{\partial T_1}{\partial x} \right) + P_1 \frac{\partial v}{\partial x} = Q_{12}(T_1, T_2), \quad (2)$$

$$\rho \dot{E}_2(x_0, t) - \frac{\partial}{\partial x}\left(\kappa_2 \frac{\partial T_2}{\partial x} \right) + P_2 \frac{\partial v}{\partial x} = -Q_{12}(T_1, T_2). \quad (3)$$

It is important to note that the addition of any thermodynamically balanced and temperature independent term

$$E \Rightarrow E + E_{\mathrm{add}}(\rho), \quad P \Rightarrow P + P_{\mathrm{add}}(\rho), \quad P_{\mathrm{add}} = -\mathrm{d}E_{\mathrm{add}}/\mathrm{d}V = \rho^2 \mathrm{d}E_{\mathrm{add}}/\mathrm{d}\rho \quad (4)$$

does not change the heat balance equation. Since the equations of dynamics (see below) includes totals for the both subsystems, the addition of such a contribution to one subsystem while subtracting for another identity retains all of the equations. This allows one of the subsystems going to that a purely thermal contribution vanishes, when appropriate temperature vanishes:

$$F_2(\rho, T_2) \Rightarrow F_2(\rho, T_2) - F_2(\rho, 0), \quad F_1(\rho, T_1) \Rightarrow F_1(\rho, T_1) + F_2(\rho, 0) = F(\rho, T_1, 0). \quad (5)$$

In the majority of metals, a variation of the electron temperature does not exert influence upon the properties of the phonon subsystem and a variation of the ion (phonon) temperature does not influence the electronic properties. This assumption is used in many quantum mechanical calculations of electronic properties of metals. It is valid to a good accuracy in the case of simple and noble metals. In particular, for silver and gold which are studied below this assumption is true, so T_{i} and T_{e} are proper orthogonal temperatures.

The electron–phonon energy exchange is described by the equation

$$Q_{\mathrm{ei}}(\rho, T_{\mathrm{e}}, T_{\mathrm{i}}) = \alpha(\rho, T_{\mathrm{e}})(T_{\mathrm{e}} - T_{\mathrm{i}}). \tag{6}$$

It is easy to see that in the substantially two-temperature case $T_{\mathrm{e}} \gg T_{\mathrm{i}}$ one can neglect the ion (phonon) temperature as compared to the electron temperature and assume:

$$Q_{\mathrm{ei}}(\rho, T_{\mathrm{e}}, T_{\mathrm{i}}) \approx Q_{\mathrm{ei}}(\rho, T_{\mathrm{e}}, 0) = \alpha(\rho, T_{\mathrm{e}})T_{\mathrm{e}} \approx \alpha(\rho, T_{\mathrm{e}})(T_{\mathrm{e}} - T_{\mathrm{i}}), \tag{7}$$

where, by definition in this case, $\alpha(\rho, T_{\mathrm{e}}) = Q_{\mathrm{ei}}(\rho, T_{\mathrm{e}}, 0)/T_{\mathrm{e}}$ for arbitrary dependence on the electron temperature and density. In the opposite case, when T_{e} and T_{i} are close to each other, equation (6) may be considered as the first term of the expansion in terms of small difference $(T_{\mathrm{e}} - T_{\mathrm{i}})$.

Thus system of the equations of two-temperature (2T) hydrodynamics is written down in the form

$$\rho \dot{v}(x_0, t) = -\frac{\partial P}{\partial x}, \tag{8}$$

$$\rho \dot{E}_{\mathrm{e}}(x_0, t) = \frac{\partial}{\partial x}\left(\kappa_{\mathrm{e}}\frac{\partial T_{\mathrm{e}}}{\partial x}\right) - P_{\mathrm{e}}\frac{\partial v}{\partial x} - \alpha(T_{\mathrm{e}} - T_{\mathrm{i}}) + Q, \tag{9}$$

$$\rho \dot{E}_{\mathrm{i}}(x_0, t) = \frac{\partial}{\partial x}\left(\kappa_{\mathrm{i}}\frac{\partial T_{\mathrm{i}}}{\partial x}\right) - P_{\mathrm{i}}\frac{\partial v}{\partial x} + \alpha(T_{\mathrm{e}} - T_{\mathrm{i}}). \tag{10}$$

The continuity equation $\rho\partial x = \rho_0\partial x_0$, where ρ, ρ_0 are current and the initial density, is satisfied automatically in Lagrangian coordinates, $E_{\mathrm{e}}, E_{\mathrm{i}}$ are the specific electron and ion energy, κ is thermal conductivity coefficient, α is the electron–ion (electron-lattice) heat exchange coefficient.

Despite the short duration of 2T stage its consideration appears essentially important. At this stage, the thermal profile that defining all further dynamics is formed. At $T_{\mathrm{e}} \gg T_{\mathrm{i}}$, thermal conductivity of the electronic subsystem is much greater than the thermal conductivity of the material at equality $T_{\mathrm{e}} = T_{\mathrm{i}}$. Due to this the thickness of a heated layer $d_{\mathrm{t}} \sim \sqrt{\kappa_{\mathrm{e}}/\alpha}$ in thick targets appears much more, than depth of absorption of radiation (skin-layer). In the thin films (film thickness $d \ll d_{\mathrm{t}}$) considered below, in time of 2T stage the electron temperature has time to be leveled practically on all thickness of a film. As a result further dynamics weakly depends on which side of the heating is carried out, and on the characteristics of heating pulse. Initial electron temperature jump occurs on 2T stage and cannot be correctly described without its consideration.

For the ionic subsystem (lattice) semiempirical equations of state (EOS) without the thermal electronic contribution for silver and gold, similar to described in [14, 15] were used. For electron subsystem the EOS and the coefficient of thermal conductivity were taken the analytical approximations built on the frame of the quantum-mechanical modeling [16–19]. Ion (phonon) thermal conductivity is considerable less and is neglected. For the glass, an approximation of the principal Hugoniot of Pyrex [20] was used.

2.1. Elastic shear stress
At the calculations of the oscillatory mode in a gold film (section 3) the contribution of elastic shear stresses was in addition considered. This is necessary to get the correct speed of sound and shock waves [21–23]. In the case of uniaxial motion it is necessary, for this purpose, to add S_{xx} to hydrostatic pressure P, defined by EOS, with the corresponding additive in energy:

$$
\begin{aligned}
P &\Rightarrow P_{xx} = P(\rho, T_{\mathrm{i}}, T_{\mathrm{e}}) - S_{xx}, \quad S_{xx} = (4G/3)\partial\xi/\partial x, \quad \xi = x - x_0, \\
E &\Rightarrow E(\rho, T_{\mathrm{i}}, T_{\mathrm{e}}) + (4G/3)(\partial\xi/\partial x)^2/(2\rho).
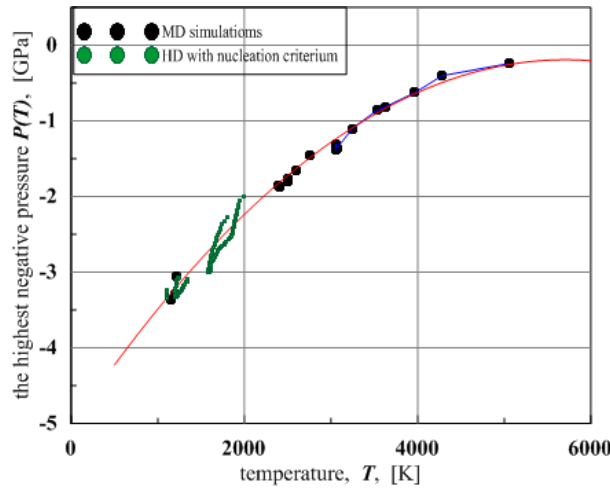\end{aligned} \tag{11}
$$

Figure 1. Moments of break at the molecular dynamics simulation (MD, black circles) and the hydrodynamic calculation (HD, green circles) with criterion of nucleation, equation (12).

Here G is the shear modulus. In the solid phase, it is necessary to add S_{xx} to the pressure in equation (8). Thus effective compression modulus is increased by $(4/3)G$, the material becomes harder and speed of a sound increases. In the heat balance equation (10), such addition to the energy and pressure identically cancel as any independent of temperature thermodynamically consistent additive. Upon melting, shear elasticity disappears and the associated energy is converted into the energy of the ion subsystem that accelerates melting. As shown in section 3, without this term, a wrong sound speed and so a wrong period of oscillations is obtained.

2.2. Nucleation criterion of break up
In section 4, for breaking of the film, nucleation criterion applies [24]:

$$\tau_{\text{nucl}} \geqslant \frac{\eta(-P)}{V(\rho/m_{\text{at}})^2 \sigma \sqrt{k_{\text{B}} T_{\text{i}} \sigma}} \exp \frac{16\pi\sigma^3}{3k_{\text{B}} T P^2}, \quad V = \frac{4\pi}{3}(c_S \tau_{\text{nucl}})^3. \tag{12}$$

The nucleation time τ_{nucl} is taken as the smaller of the time calculated from the expansion rate $1/(-\dot\rho/\rho_0) = \partial v/\partial x_0$, and the time during which a substance is in a stretched state ($P < 0$). For the surface tension the approximation was used

$$\sigma(T_{\text{i}}) = \sigma(T_{\text{m}})\left(\frac{T_{\text{c}} - T_{\text{i}}}{T_{\text{c}} - T_{\text{m}}}\right)^{1.25}, \tag{13}$$

where T_{m} and T_{c} are the melting point and the critical temperature, respectively. Nucleation criterion (12) with such "causally-connected" volume gives the best coincidence of the moments of break at molecular-dynamic simulations and in hydrodynamic calculation with the same surface tension (figure 1) and conformity of received dependences to experimental results.

3. The oscillatory mode
The oscillatory mode of film motion is tracked on the example of calculations performed for 60 nm silver film on glass Pyrex as a substrate. Such mode arises, when the maximum stress at the film and substrate border, braking film from a substrate, remains less then the stress of adhesion which stops the separation of a film from substrate. In such situation, the film
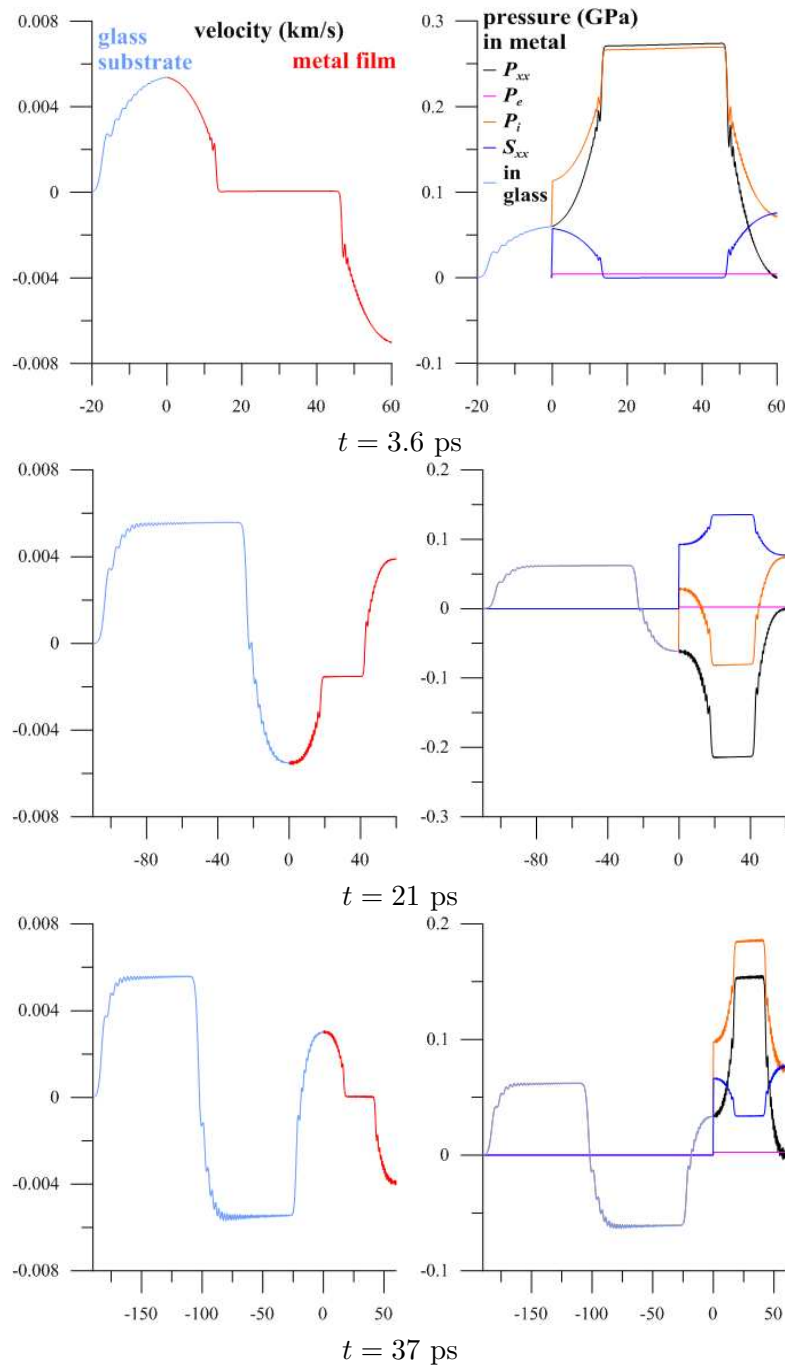
Figure 2. The oscillatory mode in silver film of 60 nm under the action of 0.7 mJ/cm^2 at some points in time (t). Profiles of velocity (km/s, left) and pressure (GPa, right) in the metal film (located on the right) and an adjacent glass substrate (located on the left). In metal, pressure is shown of ion (P_i), electron (P_e), shear stress (S_{xx}) and complete (P_{xx}); in the glass, complete pressure is shown.

movement away from the substrate is replaced by the movement to the substrate, etc (figures 2 and 3).

$F_{abs} = 0.07 \text{ mJ/cm}^2$

$F_{abs} = 0.7 \text{ mJ/cm}^2$

$F_{abs} = 0.7 \text{ mJ/cm}^2$
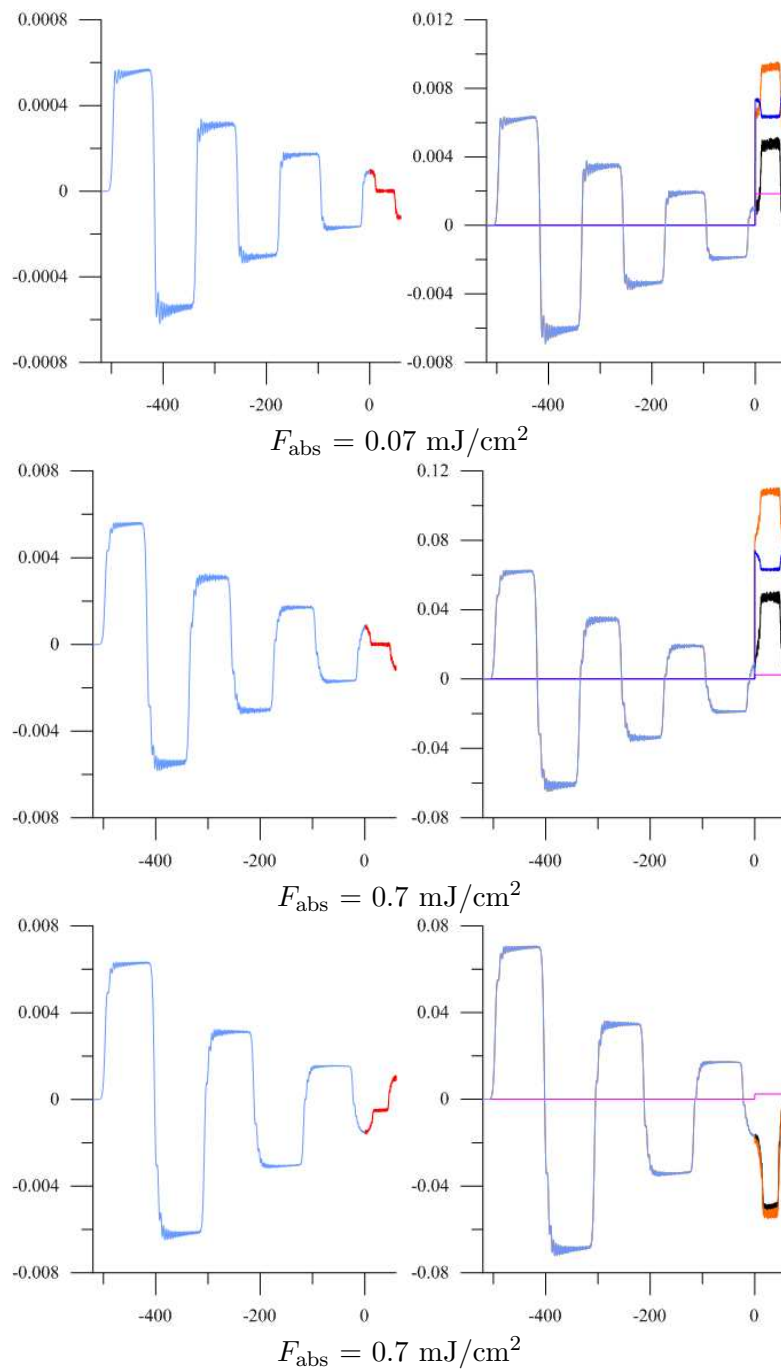
Figure 3. The oscillatory mode in silver film 60 nm thick. Profiles of the velocity (km/s, left) and pressure (GPa, right) at the time of 100 ps under the action of 0.07 mJ/cm^2 (top panel) and 0.7 mJ/cm^2 (middle panel) and under the action of 0.7 mJ/cm^2 without shear elasticity (bottom).

Oscillations are determined by passage of waves from one surface of a film to another with reflection from free surface and partial reflection from boundary with a substrate. Partial penetration of a wave into a substrate defines the attenuation of oscillations. First, on the
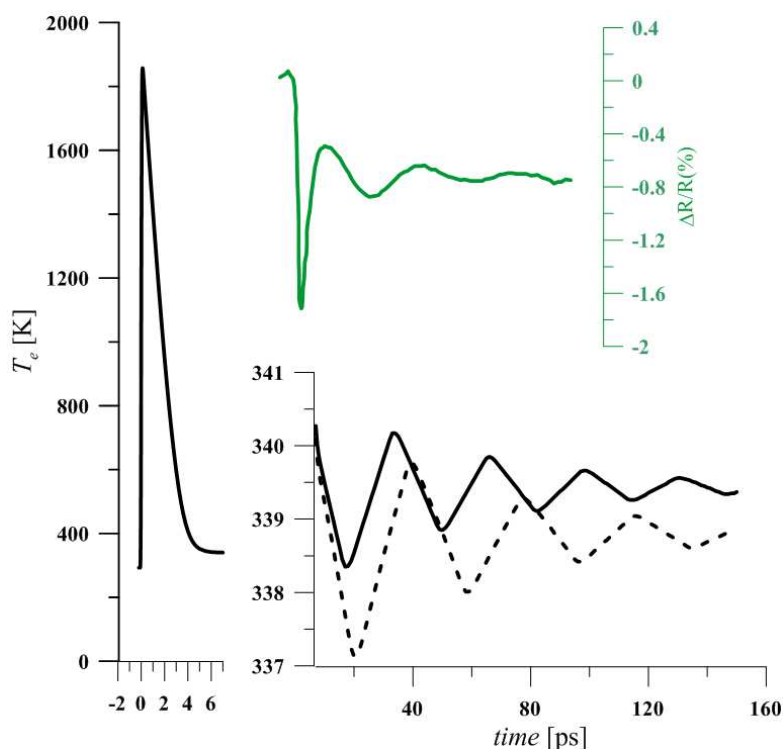
Figure 4. The oscillatory mode in silver film of 60-nm thickness. The electron temperature near the free surface under the action of 0.7 mJ/cm^2 with (solid line) and without (dashed) taking into account the elastic shear stress. The inset on a top of figure (green) shows the reflection in the experiment [25, figure 1].

boundary between the film and the substrate the compression wave comes caused by the heating of the film (see figure 2, top). Then the wave that is reflected from free surface of the film comes to the boundary as a tension wave (see figure 2, middle). After that the wave which became a tension wave having reflected (partially) from border with glass, and, having reflected from a free surface became again a compression wave reaches the border (see figure 2, bottom). This determines non-harmonic, rather trapezoidal, even close to rectangular shape of the velocity profile and pressure oscillations. The period of oscillation is determined by the passage of a sound wave across the film. Therefore the shape of the oscillations is unchanged when the absorbed energy changes, and their amplitude is practically proportional to the energy absorbed. In calculation without elastic shear stress (figure 3 bottom) the sound speed appears to be lower, and the oscillation period becomes longer. Increase and recession turn out smoother.

Disturbances of speed of substance and pressure, passing in a glass substrate, then move in it deep into with speed of a sound. Therefore presented in figure 3 instant profiles reflect time profiles of these quantities in film and substrate border.

The time profile of the electron temperature resembles a triangular wave (figure 4) and correlates well with experimental data [25]. Without the elastic shear stress (see figure 4) the oscillation period, as it was pointed out in subsection 2.1, is longer than experimentally observed. Thus the account of the elastic shear stress is crucial.

A detailed calculation of the reflection film of silver and comparison with experiment [25] is discussed elsewhere [26].
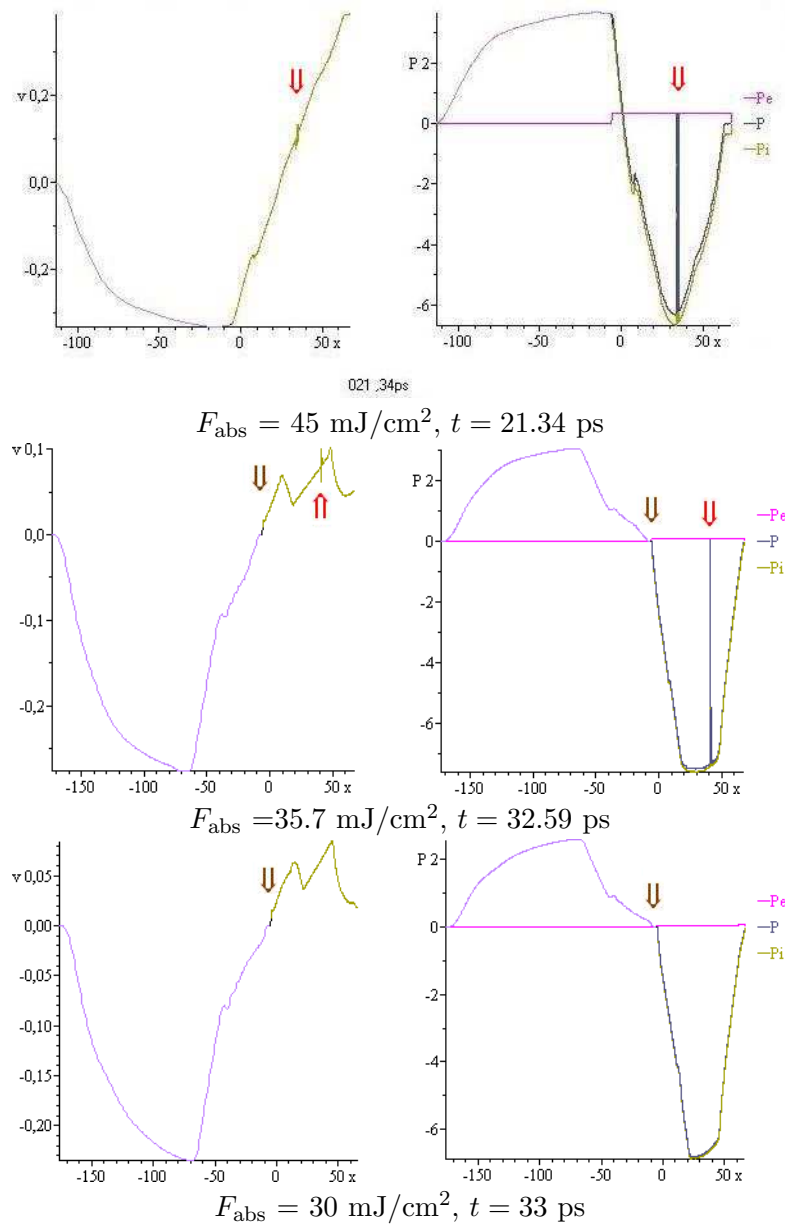
Figure 5. Delamination and break of gold film of 60 nm. The velocity (km/s) and pressure (GPa) profiles. The top panel—breaking film without delamination from the substrate at $F_{abs} = 45$ mJ/cm^2. The middle panel—delamination and a break film at $F_{abs} = 35.7$ mJ/cm^2. The lower figure–delamination of whole film at $F_{abs} = 30$ mJ/cm^2.

4. Delamination and a break of film

Delamination of the film from the substrate and its breaking when laser pulse energy increases are demonstrated with gold film on a glass substrate. Adhesion for simplicity is taken to be zero. This means that the delamination threshold turns out to be zero and the velocity of the film flying away tends to zero as the pulse energy tends to zero.

Figure 5 shows typical profiles of velocity and pressure in the film and the adjacent layer of the substrate shortly after the delamination of the film from the substrate (the lower and middle
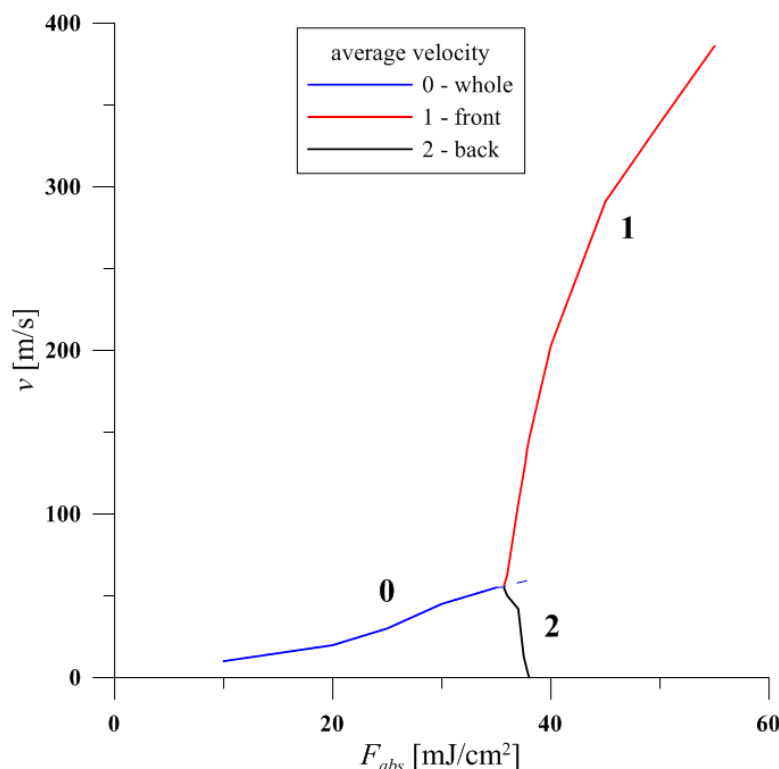
Figure 6. Average speed (speed of the center of mass) of the film as a whole—0, front flying away layer—1, and the back layer—2.

panels) and its break (upper middle panel). If fluence less than the threshold of break of the film (figure 5, bottom) it comes off as a whole. Place of the delamination is shown in the figure 5 by brown arrow. On velocity profile (left) a plateau can be seen at zero velocity in the substrate (it is located at the left) and the race of velocity going from the substrate to the flying off film. On the pressure profile (right) detachment is manifested by zero pressure between the substrate and the film. As can be seen on the profile of speed, detachment occurs when the considerable part of the film is compressed.

At a large fluence (figure 5, top) usually the film breaking (indicated by red arrows) occurs at the stage of its expansion. Thus back (adjacent to the substrate) layer moves on the substrate. After breaking off the front part of the film flies away, and back is gradually slowed down about a substrate.

More difficult is the situation at a small excess of the threshold of break (figure 5, middle). In this case, the break is delayed until a time when only in the central area of a film continues expansion, and at the periphery of it has been replaced by compression. In this case after break not only the front but also back of the film may continue moving away from the substrate.

Velocities of film (center of mass) as a whole, if the whole film is detached, of its forward flying away part if there is a break of the film, and back if it flies away from the substrate shown in figure 6.

Acknowledgments

References

[1] Zhakhovskii V V and Inogamov N A 2010 *JETP Lett.* **92** 521–526
[2] Ashitkov S I, Inogamov N A, Zhakhovskii V V, Emirov Yu N, Agranat M B, Oleinik I I, Anisimov S I and Fortov V E 2012 *JETP Lett.* **95** 176–181
[3] Inogamov N A, Petrov Yu V, Khokhlov V A, Anisimov S I, Zhakhovskii V V, Ashitkov S I, Komarov P S, Agranat M B, Fortov V E, Migdal K P, Il'nitskii D K and Emirov Yu N 2014 *J. Opt. Technol.* **81** 233–249
[4] Inogamov N A, Zhakhovsky V V, Khokhlov V A, Ashitkov S I, Emirov Y N, Khichshenko K V, Faenov A Ya, Pikuz T A, Ishino M, Kando M, Hasegawa N, Nishikino M, Komarov P S, Demaske B J, Agranat M B, Anisimov S I, Kawachi T and Oleynik I I 2014 *J. Phys.: Conf. Ser.* **510** 012041
[5] Krasyuk I K, Pashinin P P, Semenov A Yu, Khishchenko K V and Fortov V E 2016 *Laser Phys.* **26** 094001
[6] Zhakhovskii V V, Nishihara K, Anisimov S I and Inogamov N A 2000 *JETP Lett.* **71** 167–172
[7] Anisimov S I, Zhakhovskii V V, Inogamov N A and et al 2003 *JETP Lett.* **77** 606–610
[8] Anisimov S I, Zhakhovskii V V, Inogamov N A, Nishihara K and Petrov Yu V 2007 *Appl. Surf. Sci.* **253** 6390–6393
[9] Povarnitsyn M, Itina T, Sentis M, Khishchenko K and Levashov P 2007 *Phys. Rev.* B **75** 235414
[10] Upadhyay A K, Inogamov N A, Rethfeld B and Urbassek H M 2008 *Phys. Rev.* B **78** 045437
[11] Demaske B J, Zhakhovsky V V, Inogamov N A and Oleynik I I 2010 *Phys. Rev.* B **82** 064113
[12] Khokhlov V A, Inogamov N A, Zhakhovsky V V, Shepelev V V and Ilnitsky D K 2015 *J. Phys.: Conf. Ser.* **653** 012003
[13] Anisimov S I, Kapeliovich B L and Perel'man T L 1974 *Sov. Phys. JETP* **39** 375–377
[14] Khishchenko K V 2008 *J. Phys.: Conf. Ser.* **98** 032023
[15] Khishchenko K V 2008 *J. Phys.: Conf. Ser.* **121** 022025
[16] Petrov Yu V, Migdal K P, Inogamov N A and Zhakhovsky V V 2015 *Appl. Phys.* B **119** 401–411
[17] Petrov Yu V, Inogamov N A and Migdal K P 2015 *Progress in Electromagnetics Research Symposium Proc.* (PIERS) pp 2431–2435
[18] Petrov Yu V, Inogamov N A, Anisimov S I, Migdal K P, Khokhlov V A and Khishchenko K V 2015 *J. Phys.: Conf. Ser.* **653** 012087
[19] Migdal K P, Il'nitsky D K, Petrov Yu V and Inogamov N A 2015 *J. Phys.: Conf. Ser.* **653** 012086
[20] Levashov P R, Khishchenko K V, Lomonosov I V and Fortov V E 2004 *AIP Conf. Proc.* **706** 87–90
[21] Mayer A E, Khishchenko K V, Levashov P R and Mayer P N 2013 *J. Appl. Phys.* **113** 193508
[22] Khokhlov V A, Inogamov N A, Zhakhovsky V V and Anisimov S I 2013 *Physics of Extreme States of Matter—2013* ed Fortov V E *et al* (Moscow: JIHT RAS) pp 61–64
[23] Khokhlov V A, Inogamov N A, Zhakhovsky V V, Anisimov S I and Petrov Yu V 2014 *Proc. Kabardino-Balkarian State Univ.* **4**(1) 53–59
[24] Deryagin B V 1973 *Sov. Phys. JETP* **38** 1129
[25] Wang J and Guo C 2013 *Appl. Phys.* A **111** 273–277
[26] Petrov Yu V, Khokhlov V A, Inogamov N A, Khishchenko K V and Anisimov S I 2016 *J. Phys.: Conf. Ser.* This issue